

Reagentless, Ratiometric Electrochemical DNA Sensors with Improved Robustness and Reproducibility

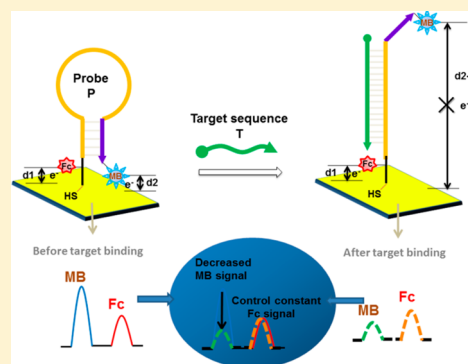
Yan Du,^{†,§} Byung Joon Lim,^{‡,§} Bingling Li,[†] Yu Sherry Jiang,[†] Jonathan L. Sessler,^{*,‡} and Andrew D. Ellington^{*,†,‡}

[†]Institute for Cellular and Molecular Biology, Center for Systems and Synthetic Biology, and Department of Chemistry, The University of Texas at Austin, Austin, Texas 78712, United States

[‡]Department of Chemistry, The University of Texas at Austin, 105 E. 24th Street - Stop A5300, Austin, Texas 78712-1224, United States

S Supporting Information

ABSTRACT: To make the electrochemical DNA sensors (E-sensor) more robust and reproducible, we have now for the first time adapted the techniques of ratiometric analyses to the field of E-sensors. We did this via the simple expedient way of simultaneously using two redox probes: Methylene blue as the reporter of the conformational change, and ferrocene as an internal control. During the conformational transduction, only the distance between the signal probe and the electrode surface undergoes an appreciable change, while the distance between the control probe and the electrode remains relatively constant. This special design has allowed very reliable target recognition, as illustrated in this report using a human T-lymphotropic virus type I gene fragment. The standard deviation between measurements obtained using different electrodes was an order of magnitude less than that obtained using a classic E-sensor, which we prepared as a control. A limit of detection of 25.1 pM was obtained with our new system, with a single mismatch discrimination factor of 2.33 likewise being observed. Additionally, this concept had general applicability, and preliminary data of a “Signal-On” ratiometric E-sensor are also provided. Taken in concert, these results serve to validate the utility of what we believe will emerge as an easily generalized approach to oligonucleotide recognition and sensing.



The ability to transduce the DNA hybridization into electrochemical signals has been greatly advanced by the development of so-called electrochemical DNA sensors (E-sensors). The E-sensors have a variety of intrinsic advantages, including high sensitivity, relatively low cost, and amenability to miniaturization and multiplexing.^{1–3} Nucleic acid analytes, including single nucleotide polymorphisms (SNPs), have been specifically detected by adapting molecular beacons⁴ to electrochemical signaling.⁵ An extremely robust and adaptable design for electrochemical signaling with molecular beacons has been developed by the Plaxco group.⁶ In this design, the distance of a redox tag to an electrode surface was altered as a consequence of nucleic acid target-induced conformational change in the molecular beacon (Scheme 1). Variations on this theme have included molecular beacon E-sensors with ferrocene (Fc),⁷ methylene blue (MB),⁸ and other redox tags;^{9,10} transduction to both reusable⁶ and disposable electrodes;¹¹ and the detection of targets ranging from short DNA^{6,9} to RNA^{12,13} to amplicons from isothermal amplification.¹⁴ To improve the sensitivity of the E-sensor, enzyme^{15,16} or nanomaterial^{17,18} amplification of the initial conformational transduction has been achieved; some of these transduction methods have allowed certain DNA targets to be detected at the attomolar level.

As with many other electrochemical biosensors, a barrier to the wider adoption of E-sensors as analytical devices are recognized problems relating to reproducibility, robustness, and reliability, which in turn stem from hard-to-avoid variations in electrode areas, DNA loading densities, and nontarget-induced reagent degradation/dissociation. This can lead to differences in the initial background currents on different sensing electrodes. The idiosyncratic background currents observed with disparate electrodes make direct determination of target binding unreliable, ultimately requiring time-consuming background scans with each new electrode or in each new analysis. Relative signal changes before and after the addition of target can be carried out for individual electrodes;^{19,20} however, such methods are inconvenient and considered impractical for potential point-of-care devices. Moreover, using such methods it is difficult to confirm whether the observed signal changes are due to target binding or deterioration of the sensing surface.

In this paper, we describe a simple ratiometric method for improving the robustness and reproducibility of E-sensors, specifically, a new “ratiometric E-sensor”. As detailed below,

Received: July 9, 2014

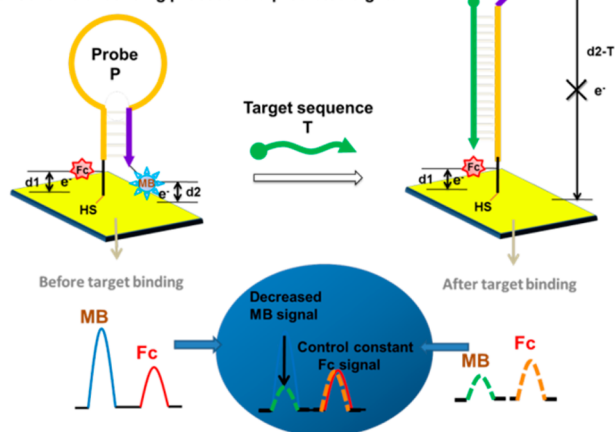
Accepted: July 10, 2014

Published: July 10, 2014

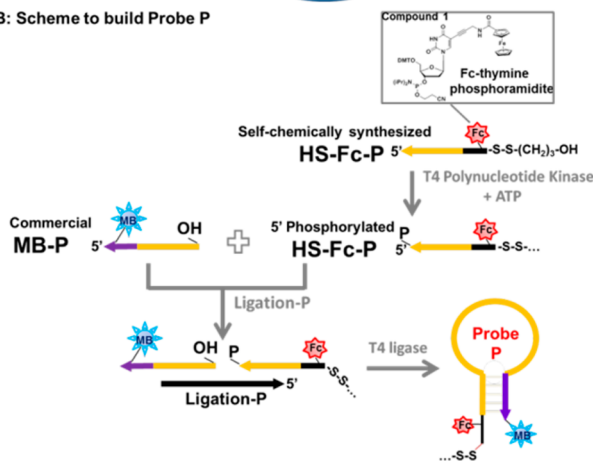
Scheme 1. Schematic View of the Present E-DNA Sensor That Relies on a Ratiometric Reporter^a

E-DNA sensor with internal control ratio-metric reporter (R-E-DNA sensor)

A: Scheme of sensing process and predicted signal



B: Scheme to build Probe P



^a(A) Mechanism of transduction. (B) Construction of Probe P from MB-P and HS-Fc-P. After hybridization to a complementary strand, Ligation-P, the phosphorylated HS-Fc-P and MB-P were ligated together by T4 DNA ligase.

we build on the basic Plaxco's E-sensor approach, starting from their first "Signal-Off" strategy. We have done so because such E-sensors are reagentless and thus excellent candidates for the development of point-of-care diagnostics.^{8,19,21} However, the inclusion of the two redox components uniquely addresses the shortcomings noted above, especially in relation to variations that arise from different DNA loading densities and nontarget-induced reagent degradation/dissociation. The ratiometric E-sensor we describe here is expected to be general and thus readily extrapolated to create a range of other oligonucleotide electrochemical DNA or aptamer-based biosensors that rely on the same or other conformational transduction principles.^{3,22–25} Support for this contention comes from a demonstration that it may also be used effectively for "Signal-On" sensing.

RESULTS AND DISCUSSION

The ratiometric method we describe here is based on the use of two electrochemical probes in parallel. In addition to the classic signal probe (MB) found in other E-sensors, we have included another redox probe, Fc, as a control. The design principle is that, during target-induced conformational transduction, only the distance between the signal probe (MB) and the electrode

will be changed, while the relative distance between the control probe (Fc) and the electrode should remain constant. Therefore, the control probe is expected to serve as an internal control.

To demonstrate the utility of our ratiometric standardization, we designed a "Signal-Off" E-DNA sensor⁶ similar to one reported previously by Plaxco and co-workers. However, in addition to adding a second redox component, we changed the target sequence so as to detect sequences present in the human T-lymphotropic virus type I gene (Target T).²⁶ As shown in Scheme 1, a 37-mer molecular beacon (Probe P) was immobilized on a hand-polished gold disk electrode via a 3' thiol (Scheme 1A). Probe P was constructed by enzymatically ligation of an HS- and Fc-labeled oligonucleotide (HS-Fc-P) with a MB-labeled oligonucleotide (MB-P). HS-Fc-P was synthesized using a commercial 3'-thiol modifier solid phase column and a Fc-modified thymidine (T) phosphoramidite (compound 1) (Scheme 1B; see the Supporting Information for characterization and experimental details). MB-P was obtained from a commercial supplier.

As shown in Scheme 1A and Figure 1, in the absence of the target, both the Fc and MB tags are held in proximity to the electrode and yield effective electron transfer signals at 0.440 and -0.265 V (vs Ag/AgCl, Two M NaCl), respectively. The Fc probe was chosen because its E^0 is well-separated from

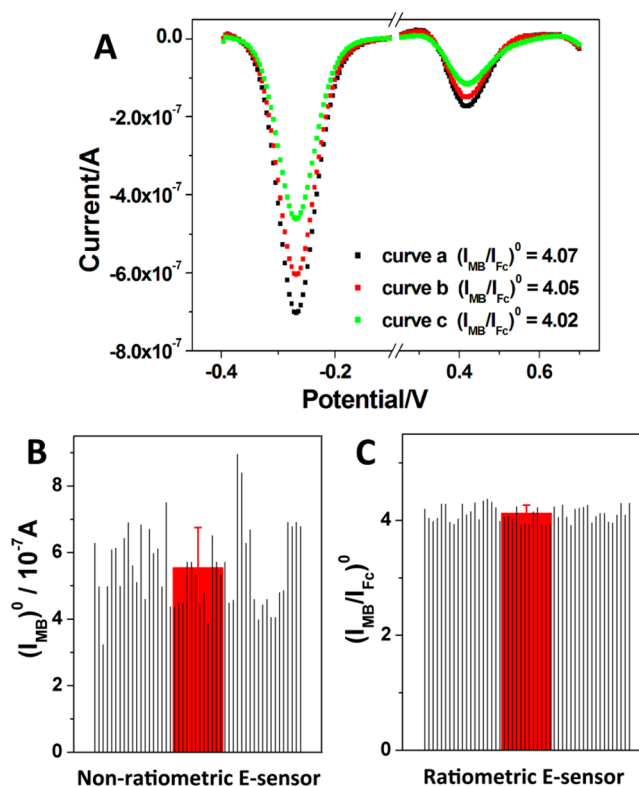


Figure 1. Comparison between non-ratiometric and ratiometric E-sensors. (A) Typical SWV curves scanned prior to target binding on three different sensing electrodes. (B) Reproducibility of the non-ratiometric E-sensor. (C) Reproducibility of the ratiometric E-sensor. Throughout, $(I_{MB})^0$ refers to the initial background response of MB prior to target binding. $(I_{MB}/I_{Fc})^0$ refers to the initial background ratio of MB and Fc signals prior to target binding. The black histograms represent the background responses of 50 individual measurements over eight electrodes. Average values are represented by the red bars. The error bars in the red histograms represent the SD for 50 individual measurements.

that of MB. Figure 1 shows square wave voltammetry (SWV) curves from three different electrodes. As hypothesized, under standard experimental operation, irrespective of differences in electrode areas, probe densities, or idiosyncracies of cleaning, the background current ratio between MB and Fc was generally the same on each sensing surface.

To confirm that the ratiometric E-sensor (containing both MB and Fc) is highly reproducible relative to the non-ratiometric E-sensor (containing only MB), the initial background SWV peak currents of MB ($(I_{\text{MB}})^0$) and Fc ($(I_{\text{Fc}})^0$) and the initial background current ratios of ($(I_{\text{MB}}/I_{\text{Fc}})^0$) before target detection were collected over 50 individual measurements (Figure 1B and C). These data were obtained using eight electrodes, including the same electrodes on different days and different electrodes on the same day. Similar to the classic E-sensor, the background (I_{MB}^0) response in these 50 tests showed wide variation (Figure 1B) with an average (standard deviation, SD) of 5.54×10^{-7} A and a variance of 1.21. However, in our ratiometric E-sensor the variation in background signal was significantly reduced ($(I_{\text{MB}}/I_{\text{Fc}})^0$; Figure 1C) with an average background ratio response of 4.13 and a variance of 0.14. The ratiometric approach was far more robust, reliable, and reproducible than the previous approach that relied on electrochemical “absolute values”.

In response to the target sequence (Target T, at, e.g., 500 nM), the Probe P undergoes a conformational change due to formation of a P-T duplex. While the Faradaic current from the 3' Fc tag was almost unchanged (presumably since its distance to the electrode, d1 remained unchanged), the 5' MB tag showed a sharp decrease in current, consistent with it being further away from the electrode (d2 goes to d2-T) (Scheme 1A and Figure 2).

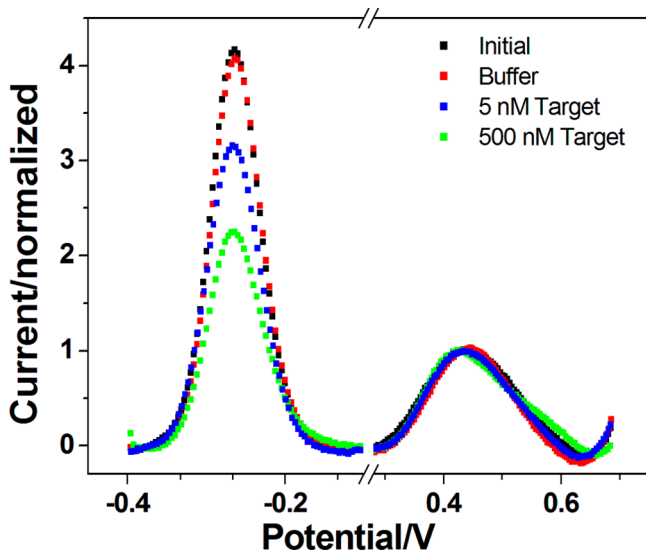


Figure 2. Typical SWV curves as obtained before and after target binding. The peak current from Fc is normalized for each curve.

In order to confirm that electrochemical signals were due to nucleic acid hybridization and conformational changes rather than other unattributed effects, the behavior of Probe P was analyzed using native polyacrylamide gel electrophoresis (PAGE) (Figure 3). As can be seen from inspection of Figures 3A (using unlabeled Probe P and Target T) and 3B (using MB- and Fc-labeled Probe P and Target T), a higher band was observed only in the presence of Target T (lanes 2–4, 8, and 9). Moreover, the density of this band was in direct proportion to

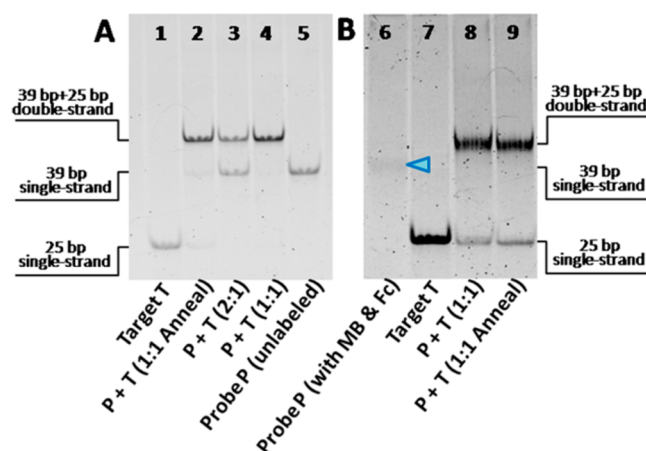


Figure 3. Gel electrophoresis of E-sensor conformational transitions. Samples were developed on a 12% native PAGE. (A) Unlabeled Probe P, lane 1: [T] = 100 nM; lanes 2 and 4: [P] = [T] = 100 nM; lane 3: [P] = 2[T] = 100 nM; lane 5: [P] = 100 nM. (B) HS- and Fc- and MB-labeled Probe P, lane 6: [P] = 200 nM; lane 7: [T] = 200 nM; lanes 8 and 9: [P] = [T] = 200 nM. The mobilities of the different conformers are indicated at the sides of the gels. The arrow indicates a faint band, as described in the text.

the target added. Interestingly, the presence of one or both electrochemical tags on Probe P reduced SYBR Gold staining fluorescence (blue arrow in Figure 3B, lane 6). Nevertheless, evidence for hybridization between Probe P and Target T was observed (Figure 3B, lanes 8 and 9). In addition to electrophoresis, cyclic voltammetry (CV) and chronocoulometry (CC) were used to validate the addition of, and changes to, molecules during the sensor fabrication and detection process (Figure S3 in the Supporting Information).

A dose–response curve was prepared for the ratiometric E-sensor by monitoring the SWV peak current ratio between the MB current and the Fc current ($I_{\text{MB}}/I_{\text{Fc}}$) after Target T detection. Such analyses provide a complement to measurements of the absolute MB current value (I_{MB}) or the relative current ($(I_{\text{MB}}/I_{\text{MB}})^0$). They are attractive because they are potentially more reproducible. To construct these curves, data were collected using different electrodes. As can be seen from an inspection of Figure 4A and B, the response varied in a log–linear fashion with the target concentration, as expected. Target T concentrations from 50 pM to 1 μ M could be measured, with the highest ratio signal suppression being around 50% from the background and an overall $R^2 = 0.997$. The detection limit (LOD) at a signal-to-noise ratio of 3 was calculated to be 25.1 pM, comparable with the non-ratiometric or classic E-DNA sensor.⁶ However, in contrast to this latter classic approach, control studies carried out using just the signal probe MB (I_{MB}) revealed relatively large standard deviations and an overall R^2 of 0.958, although peak current suppression with increasing target concentration was seen (Figure 4C and D). The lower reliability observed with the control system is ascribed to the variance in the background signal (I_{MB}^0) discussed above (cf. Figure 1B).

To ensure that the signals observed were due to the specific hybridization of Target T to the probe sequence (Probe P), a series of control experiments were carried out with non-complementary DNA (Non-T), and with targets containing 1–4 mismatches (T-SNP1, T-SNP2, T-SNP3, and T-SNP4). The targets that contained three or more mismatches produced no observable interactions with Probe P, while single and double mismatches gave signals smaller than the completely matched

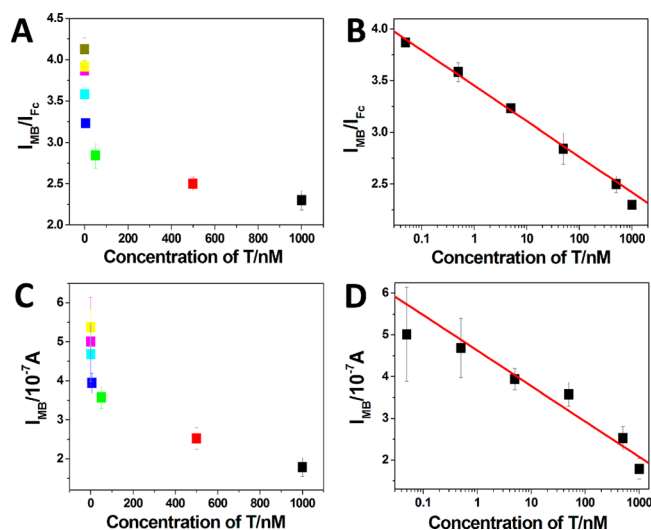


Figure 4. Concentration dependence of Target T as observed using ratiometric E-sensors and non-ratiometric E-sensors. (A) Concentration dependence of Target T based on the ratio I_{MB}/I_{Fc} . (B) Concentration dependence of Target T represented by a log-linear plot of I_{MB}/I_{Fc} . (C) Concentration dependence of Target T based on I_{MB} . (D) Concentration dependence of Target T represented by log-linear plot of I_{MB} . The error bars are standard deviations of measurements based on three independent experiments.

target (Figure 5A). As with non-ratiometric E-sensors, it is anticipated that long targets will yield larger signal changes than shorter targets, but that the specificity of long targets will be poorer than that of shorter targets.²⁷

More quantitatively, the single-base mismatch discrimination factor can be defined as the ratio of the decrease in signal with a perfectly paired target ($\Delta I_{MB}/I_{Fc}$) versus that seen with a mismatched target. The larger the discrimination factor, the better the specificity for single-base mismatch will be. The discrimination factor for the single-base mismatched sequence T-SNP1 was 1.60 at 25 °C. Increasing the temperature should increase the level of discrimination.^{28,29} In the present instance, increasing the temperature to 37 °C, resulted in a discrimination value of 2.50 (Figure 5B). These latter values are comparable to those obtained with E-sensors,⁷ where a discrimination factor of 2.33 was noted. However, our internally controlled, double redox sensor shows mismatch discrimination comparable to those of fluorescence methods (discrimination factor of 2.18),³⁰ and somewhat better than those of similar experiments that have been reported in the context of electrochemistry (1.67),³¹ colorimetry (1.33),³² surface plasmon resonance (1.67),³³ quartz crystal microbalance (1.22),³³ or surface-enhanced Raman scattering (1.33) sensing.³⁴ Based on prior studies, it is anticipated that additional mutation discrimination could likely be obtained by manipulating salt concentrations and other buffer components.³⁵ Optimization efforts along these latter lines are in progress.

Notably, the HS-Fc-P used in the “Signal-Off” ratiometric E-sensor contained four Fc labels to ensure an adequate peak current signal during the SWV scan. While SWV scans are fast (they can be carried out within 10 s), typically they give rise to relatively decreased peak currents as the result of mainly the high charging/background current (near E_0 of Fc) required. Alternatively, if alternating current voltammetry (ACV) or differential pulse voltammetry (DPV) techniques are employed, a much slower scan rate (see Experimental Section) can be

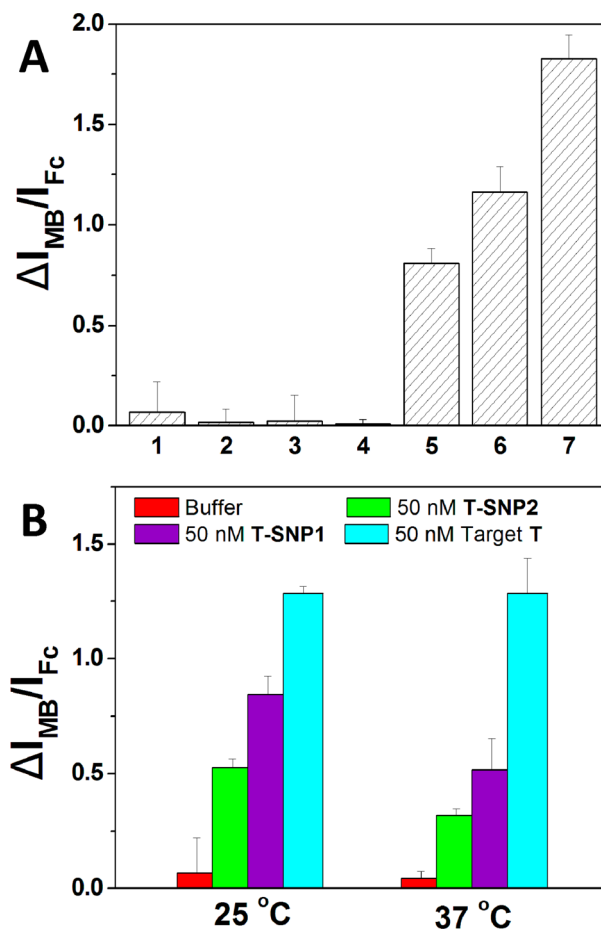


Figure 5. Selectivity of the ratiometric E-sensor. (A) Transduction by Probe P with a series matched and mismatched targets at 25 °C. Buffer only (1), 1 μ M Non-T (2), 1 μ M T-SNP4 (4 mismatches) (3), 1 μ M T-SNP3 (3 mismatches) (4), 1 μ M T-SNP2 (2 mismatches) (5), 1 μ M T-SNP1 (1 mismatch) (6), and correctly paired Target T (7). (B) Selectivity at different temperatures. T-SNP1 and T-SNP2 contain 1 and 2 mismatches relative to Target T, respectively.

accommodated, as shown in Figure 6A below. However, upward of 5 min is required for each scan.

We have also carried out additional experiments to show the utility of the present ratiometric approach in the context of a “Signal-On” E-sensor. The basic sensor design was the same as has been previously demonstrated (Figure 6A), except that a Fc label was covalently added to the 3' end of Probe ON-P2. To also demonstrate the facility with which ratiometric sensors can be generated, the dual-labeled Probe ON-P2 oligonucleotide was not synthesized in house. Rather, it was ordered directly from Biosearch Technologies. The generality of the ratiometric approach was further emphasized by using ACV for measurements rather than SWV.

Briefly, MB- and Fc-labeled Probe ON-P2 was hybridized with Probe SH-ON-P1 that had been preimmobilized on the gold surface, leaving a loop in the middle of the duplex. Target sequence (Target ON-T) can bind the loop sequence thereby triggering a strand displacement reaction that releases the MB-labeled 5' terminal of Probe ON-P2. Since the released MB has more chances to approach the gold surface, the MB signal increases. However, the relative distance between the immobilized Fc label and the electrode does not change as the result of this release. Therefore, readings from the Fc subunit serve as an

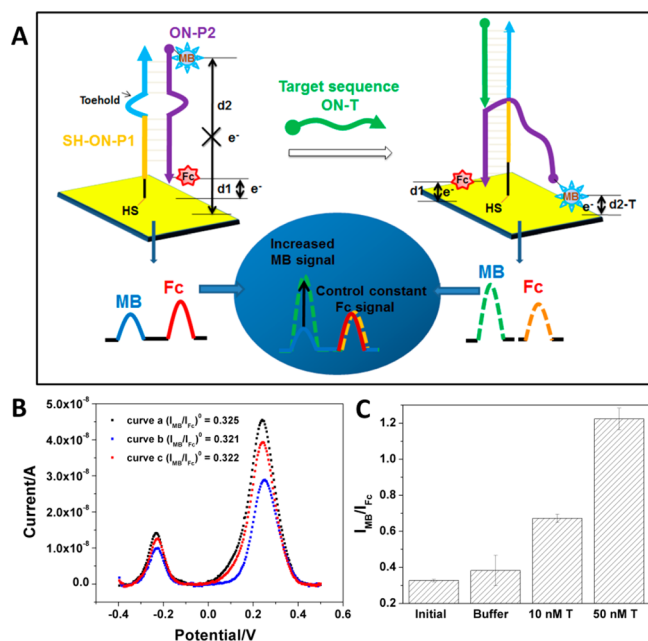


Figure 6. (A) Schematic view of a “Signal-On” E-DNA sensor that relies on a ratiometric reporter. (B) Typical ACV curves scanned prior to target binding on three different sensing electrodes for the “Signal-On” ratiometric E-sensor. (C) I_{MB}/I_{Fc} response obtained before (buffer, negative control) and after target binding.

unmodulated internal control. This permits ratiometric sensing and its attendant advantages in terms of sensitivity and reproducibility.

In general, the present ratiometric “Signal-On” E-sensor proved much more robust, reliable, and reproducible than sensors that relied on the peak current alone as a read out indicator. Different electrodes gave different I_{MB}^0 values (see Figure 6B for examples). The average value of I_{MB}^0 for eight different electrodes was 1.254×10^{-8} A with a variance (SD) of 0.286. In contrast, the average value of $(I_{MB}/I_{Fc})^0$ for eight different electrodes was much more reliable, 0.320 with a variance of 0.013. Moreover, because the signal gain is no longer limited by background current, exposure to 10 nM of the target produced a near 100% signal increase in I_{MB}/I_{Fc} over $(I_{MB}/I_{Fc})^0$ (Figure 6C). The ratiometric “Signal-Off” E-sensor 10 nM target produced about a 25% signal decrease in I_{MB}/I_{Fc} .

CONCLUSIONS

In conclusion, we have developed a novel ratiometric method that greatly improves the performance of E-sensors. By importing an internal control redox probe into the sensing platform, we have overcome a disadvantage of electrochemical DNA sensors, namely, irreproducibility, and have done so without loss of sensitivity or selectivity. An additional potential advantage of the MB/Fc approach detailed here is that the current ratio prior to target binding can be used as a positive control to validate electrode function. This is useful since drastic variations in the baseline ratio over time can be indicative of a faulty electrode.

It is likely that this advance can also be applied to other types of E-sensors, including those based on aptamer refolding in the presence of a ligand.^{3,22,23,25,36–40} Efforts are currently being made to extrapolate the present approach in such directions. The key point is that, in any configuration, the analyte-dependent signal can be read out directly by simply calculating the current ratio between MB and Fc (or some other appropriate redox probe). In other words, even if the change in the relative current response cannot be readily predicted (or correlated accurately with target concentration), the change in the current ratio will be indicative of target binding. We thus deem the approach described here as useful and attractive as a potentially generalizable approach to oligonucleotide sensor development.

EXPERIMENTAL SECTION

Materials. All solvents and chemicals used for the synthesis of compound 1 (Fc-T-phosphoramidite) were purchased from Sigma-Aldrich (St. Louis, MO) and Acros Organics (Morris Plains, NJ) and used without further purification. TLC analyses were carried out using Sorbent Technologies silica gel (200 μ m) sheets. Column chromatography was performed on Sorbent Technologies silica gel 60 (40–63 μ m). NMR solvents were purchased from Cambridge Isotope Laboratories (Tewksbury, MA). All other phosphoramidites and materials used for solid phase oligonucleotide synthesis were purchased from Glen Research (Sterling, VA). The methylene-blue-labeled probe (MB-P) was ordered from Biosearch Technologies (Novato, CA). All other unmodified nucleotides were ordered from Integrated DNA Technology (Coralville, IA). Oligonucleotide sequences are summarized in Table 1. T4 polynucleotide kinase (T4 PNK) and T4 DNA ligase were ordered from New England BioLabs Inc. (Ipswich, MA). SYBR Gold was purchased from Life Technologies (Grand Island, NY). All DNA samples and

Table 1. Sequence of Oligonucleotides Used in This Work

name	sequence	5' modification	3' modification
unlabeled Probe P	5'-TTTGAGTATTCCTCCAGGCCATGCGCAAATACTCTTTT-3'		
MB-P	5'-TTTGAGTATTCCTCCAGG-3'	methylene blue	
HS-Fc-P	5'-CCATGCGCAAATACTCT(Fc)T(Fc)T(Fc)T-3'		thio C3
Ligation-P	5'-ATTTGCGCATGGCCTGGAGGAATAC-3'		
Target T	5'-GAGTATTTGCGCATGGCCTGGAGGA-3'		
T-SNP1	5'-GAGTATTTGCGCATGGCCTGTAGGA-3'		
T-SNP2	5'-GAGTATTTCCGCATGGCCTGTAGGA-3'		
T-SNP3	5'-GAGTATTTCCGCATGGCCAGTAGGA-3'		
T-SNP4	5'-GAGTATTTCCGCTTGGCCAGTAGGA-3'		
Non-T	5'-AACCAGCCAGTGAGCCAATTCATGA-3'		
Probe SH-ON-P1	5'-GCGAGTTAGACCGATCCCCCCTTCGTCCAGTCTTTT-3'	thio C6	
Probe ON-P2	5'-GACTGGACGCCCCCATCGGTCTAACTCGCT(Fc)T-3'	methylene blue	
Target ON-T	5'-AAAAGACTGGACGAA-3'		

6-mercaptohexanol (MCH) were dissolved in phosphate-buffered saline (10 mM PBS, 500 mM NaCl, 2.7 mM KCl, pH 7.4) and stored at 4 °C before use. All other chemicals were purchased from Sigma-Aldrich (St. Louis, MO) as analytical grade.

Instruments. Square wave voltammetry was performed with a model CH Instrument 660E electrochemical workstation (CH Instruments, Inc., Austin, TX). A conventional three-electrode system with a Au electrode (1.2 mm in diameter) as the working electrode, a Ag/AgCl electrode as the reference electrode, and a platinum wire as the counter electrode was used. CVs were performed in a solution of 5 mM $K_4[Fe(CN)_6]/K_3[Fe(CN)_6]$ (in 20 mM Tris-HCl, 500 mM NaCl, 5 mM KCl, pH 7.4). CCs were performed in a solution of 0.05 mM $[Ru(NH_3)_6]^{3+}$ (RuHex, in 10 mM Tris-HCl, pH 7.4). SWV and ACV were performed in 10 mM PBS, 500 mM NaCl, 2.7 mM KCl, pH 7.4. The SWV parameters adopted were as follows: Increment potential was 4 mV, amplitude was 25 mV, frequency was 50 Hz, and voltage range was from -0.4 to 0.7 V. The ACV parameters adopted were as follows: Increment potential of 4 mV, amplitude of 25 mV, frequency of 10 Hz, and voltage range of -0.4 to 0.6 V. All the measurements were carried out at room temperature (ca. 25 °C). Hybridization reactions were developed on a 12% native polyacrylamide gel: a 20 μ L aliquot of the hybridization solution was mixed with 6 μ L of 6 \times Loading Dye (50% glycerol spiked with a small amount of the dye Orange G) and loaded on the polyacrylamide gel. The gel was developed at 250 V at room temperature, followed by SYBR Gold staining. Bands were observed and quantitated using a Storm Scanner 840 instrument (GE Healthcare Life Science, Pittsburgh, PA). NMR spectra for the synthesis of compound 1 were recorded on Varian Direct Drive 400 MHz and Varian MR 400 MHz instruments, and the electrospray ionization (ESI) mass spectra were recorded on an Agilent Technologies 6530 Accurate Mass QTOF/MS apparatus. Cyclic voltammetry was performed on a CV-50W Voltammetric Analyzer (Bioanalytical Systems Inc., West Lafayette, IN).

Synthesis of Compound 1 (Fc-T-phosphoramidite). The synthesis scheme, characterization, and other experimental details are provided in the Supporting Information.

Synthesis of HS-Fc-P. Synthesis of the oligonucleotide HS-Fc-P was performed on a commercial Expedite 8909 nucleic acid synthesizer with a 0.2 μ mol 3'-thiol-modifier C3 S-S CPG support column. A standard oligodeoxynucleotide synthesis protocol was used except that coupling times were extended (to 15 min) and a more concentrated phosphoramidite solution (0.2 M) was employed with compound 1. The product was deprotected and purified using a Glen-Pak DNA Purification Cartridge, and the detailed procedure provided by the Glen Research Company (http://www.glenresearch.com/Technical/GlenPak_UserGuide.pdf).

Phosphorylation of HS-Fc-P. The phosphorylation of HS-Fc-P was performed in 1 mL of T4 ligase buffer (50 mM Tris-HCl, 10 mM $MgCl_2$, 1 mM ATP, 10 mM DTT, pH 7.5) solution containing 100 μ M HS-Fc-P and 50 μ L of T4 PNK (10 000 units/mL). The mixture was incubated at 37 °C for 3 h. The solution was then incubated at 65 °C for 20 min to denature the enzyme. After precipitation with ethanol, the DNA was dissolved in 90 μ L of DI water. A G25 column was used to remove residual salts, and 90 μ L of 558 μ M 5'-phosphorylated HS-Fc-P was obtained for subsequent ligation reactions.

Ligation of MB-P to Phosphorylated HS-Fc-P. The MB-P and 5'-phosphorylated HS-Fc-P was ligated together

with T4 DNA Ligase. Four tubes were prepared with that contained 80 μ M phosphorylated HS-Fc-P, 30 μ M MB-P, 30 μ M Ligation-P (see also Scheme 1), and 1 \times ligation buffer for a total of 100 μ L per tube. These samples were incubated for 5 min at 80 °C and cooled down to 25 °C at a rate of 0.1 °C/s. After this first incubation was deemed complete, 20 μ L of 120 000 units of T4 DNA ligase in 1 \times ligation buffer was added to each tube for a total of 120 μ L per tube. The reaction mixture was further incubated at 16 °C for 16 h, followed by incubation at 65 °C for 20 min. After incubation, Probe P was purified on a 12% denaturing PAGE gel (7 M urea, 1 \times TBE), and its final concentration was confirmed by absorption determinations with a Nanodrop ND-1000 spectrophotometer (Wilmington, DE, USA).

Sensing Platform Fabrication. To cleave the S-S of thiol-tagged Probe P, 3 μ L of 16.3 μ M Probe P was mixed with 4.8 μ L of 100 mM tris(2-carboxyethyl)phosphine (TCEP), and this solution was incubated in the dark at room temperature for 1 h. Then, 12 μ L of 2 \times PBS buffer and 4.2 μ L of DI water were added to that solution and stored at 4 °C for further use. The Au electrode was polished with 1.0, 0.3, and 0.05 μ m γ - Al_2O_3 and then washed ultrasonically with water for three cycles, followed by potential scanning in 0.1 M H_2SO_4 between -0.2 and 1.6 V until a reproducible cyclic voltammogram was obtained. The electrode was rinsed with a copious amount of water and blown dry with nitrogen before assembly. The sensing platform (Au/Probe P) was prepared by placing 4 μ L of freshly prepared Probe P (2 μ M) solution on the Au electrode and then covering the end of the electrode with a plastic cap to prevent the solution from evaporating. The assembly was kept 1.5 h at room temperature in the dark and then rinsed with PBS buffer several times. The interface was then covered with 5 μ L of 1 mM MCH (in PBS) and kept at room temperature for 30 min. After rinsing with PBS buffer, the sensing platform was stored in PBS buffer for at least 20 min prior to experimental measurements. It is worth noting that the amount of the Probe P immobilized on the electrode surface is an important factor in terms of responsivity. In our experiments, the density of Probe P on the gold electrode was calculated to be about $(2.77 \pm 0.23) \times 10^{12}$ molecules/ cm^2 , similar to values previously shown to be optimal for signaling.⁴¹

Sensing Protocol. Initial SWV signals from the MB and Fc reporters on Probe P were measured in PBS. Signals were taken after 30 min of incubation with 50 μ L aliquots of different concentrations of Target T and other sequences, as described in the text.

The Generality of the Ratiometric E-Sensor. The sensing platform (Au/Probe ON-P1-P2) was prepared by placing 15 μ L of freshly prepared Probe SH-ON-P1 (0.5 μ M, in 200 mM Tris-HCl containing 5 μ M TCEP, pH 7.4) solution on the Au electrode for 16 h at 25 °C. The resulting surface was washed with 20 mM Tris-HCl buffer, and then the modified Au electrode was treated with 1 mM MCH in 10 mM Tris-HCl buffer (pH 7.4) for 1 h. Then, 10 μ L of 2.5 μ M Probe ON-P2 (in PerfectHyb Plus hybridization buffer (Sigma, St. Louis, MO)) was placed on the Au electrode surface for 6 h to yield the final sensing platform. The sensor interface was then immersed in various concentrations of Target ON-T (in PerfectHyb Plus hybridization buffer) for 4 h at 37 °C.

■ ASSOCIATED CONTENT

Supporting Information

Synthesis of compounds 1, 3, 4, and phosphoramidite 1; cyclic voltammetry of compound 3; PAGE gel characterization and

purification of the ligation process; characterization of the sensing interface fabrication; NMR and MS spectra. This material is available free of charge via the Internet at <http://pubs.acs.org>.

AUTHOR INFORMATION

Corresponding Authors

*E-mail: sessler@cm.utexas.edu. Fax: 512-471-5009.

*E-mail: andy.ellington@mail.utexas.edu. Tel: 512 471 6445. Fax: 512 471 7014.

Author Contributions

[§]Y.D. and B.J. L. contributed equally to this work.

Notes

The authors declare no competing financial interest.

ACKNOWLEDGMENTS

This work was funded by the Welch Foundation (Grants F-1018 and F-1654 to J.L.S. and A.D.E., respectively), the Gates Foundation (OPP1028808 to A.D.E.), the National Security Science and Engineering Faculty Fellowship (FA9550-10-1-0169 to A.D.E.), and the NIH (CA 68682 to J.L.S.) The content is solely the responsibility of the authors and do not necessarily represent the official views of the sponsors.

REFERENCES

- (1) Drummond, T. G.; Hill, M. G.; Barton, J. K. *Nat. Biotechnol.* **2003**, *21*, 1192–1199.
- (2) Willner, I.; Zayats, M. *Angew. Chem., Int. Ed.* **2007**, *46*, 6408–6418.
- (3) Li, D.; Song, S. P.; Fan, C. H. *Acc. Chem. Res.* **2010**, *43*, 631–641.
- (4) Tyagi, S.; Kramer, F. R. *Nat. Biotechnol.* **1996**, *14*, 303–308.
- (5) Huang, T. J.; Liu, M. S.; Knight, L. D.; Grody, W. W.; Miller, J. F.; Ho, C. M. *Nucleic Acids Res.* **2002**, *30*, e55.
- (6) Fan, C. H.; Plaxco, K. W.; Heeger, A. J. *Proc. Natl. Acad. Sci. U.S.A.* **2003**, *100*, 9134–9137.
- (7) Immoos, C. E.; Lee, S. J.; Grinstaff, M. W. *ChemBioChem* **2004**, *5*, 1100–1103.
- (8) Xiao, Y.; Lubin, A. A.; Baker, B. R.; Plaxco, K. W.; Heeger, A. J. *Proc. Natl. Acad. Sci. U.S.A.* **2006**, *103*, 16677–16680.
- (9) Liu, G.; Wan, Y.; Gau, V.; Zhang, J.; Wang, L. H.; Song, S. P.; Fan, C. H. *J. Am. Chem. Soc.* **2008**, *130*, 6820–6825.
- (10) Wu, J. K.; Huang, C. H.; Cheng, G. F.; Zhang, F.; He, P. G.; Fang, Y. Z. *Electrochem. Commun.* **2009**, *11*, 177–180.
- (11) Jenkins, D. M.; Chami, B.; Kreuzer, M.; Presting, G.; Alvarez, A. M.; Liaw, B. Y. *Anal. Chem.* **2006**, *78*, 2314–2318.
- (12) Liu, C.; Zeng, G. M.; Tang, L.; Zhang, Y.; Li, Y. P.; Liu, Y. Y.; Li, Z.; Wu, M. S.; Luo, J. *Enzyme Microb. Technol.* **2011**, *49*, 266–271.
- (13) Yin, H. S.; Zhou, Y. L.; Zhang, H. X.; Meng, X. M.; Ai, S. Y. *Biosens. Bioelectron.* **2012**, *33*, 247–253.
- (14) Hsieh, K. W.; Patterson, A. S.; Ferguson, B. S.; Plaxco, K. W.; Soh, H. T. *Angew. Chem., Int. Ed.* **2012**, *51*, 4896–4900.
- (15) Miranda-Castro, R.; De-Los-Santos-Alvarez, P.; Lobo-Castanon, M. J.; Miranda-Ordieres, A. J.; Tunon-Blanco, P. *Anal. Chem.* **2007**, *79*, 4050–4055.
- (16) Xuan, F.; Luo, X. T.; Hsing, I. M. *Anal. Chem.* **2012**, *84*, 5216–5220.
- (17) Gao, W. C.; Dong, H. F.; Lei, J. P.; Ji, H. X.; Ju, H. X. *Chem. Commun.* **2011**, *47*, 5220–5222.
- (18) Fang, X.; Jiang, W.; Han, X. W.; Zhang, Y. Z. *Microchim. Acta* **2013**, *180*, 1271–1277.
- (19) Xiao, Y.; Lai, R. Y.; Plaxco, K. W. *Nat. Protoc.* **2007**, *2*, 2875–2880.
- (20) Bonham, A. J.; Hsieh, K.; Ferguson, B. S.; Vallee-Belisle, A.; Ricci, F.; Soh, H. T.; Plaxco, K. W. *J. Am. Chem. Soc.* **2012**, *134*, 3346–3348.
- (21) Lubin, A. A.; Plaxco, K. W. *Acc. Chem. Res.* **2010**, *43*, 496–505.
- (22) Baker, B. R.; Lai, R. Y.; Wood, M. S.; Doctor, E. H.; Heeger, A. J.; Plaxco, K. W. *J. Am. Chem. Soc.* **2006**, *128*, 3138–3139.
- (23) Mir, M.; Jenkins, A. T. A.; Katakis, I. *Electrochem. Commun.* **2008**, *10*, 1533–1536.
- (24) Gong, H.; Zhong, T. Y.; Gao, L.; Li, X. H.; Bi, L. J.; Kraatz, H. B. *Anal. Chem.* **2009**, *81*, 8639–8643.
- (25) Wu, D. H.; Zhang, Q.; Chu, X.; Wang, H. B.; Shen, G. L.; Yu, R. Q. *Biosens. Bioelectron.* **2010**, *25*, 1025–1031.
- (26) Yang, X.; Du, Y.; Li, D.; Lv, Z. Z.; Wang, E. K. *Chem. Commun.* **2011**, *47*, 10581–10583.
- (27) Lubin, A. A.; Hunt, B. V. S.; White, R. J.; Plaxco, K. W. *Anal. Chem.* **2009**, *81*, 2150–2158.
- (28) Breslauer, K. J.; Frank, R.; Blocker, H.; Marky, L. A. *Proc. Natl. Acad. Sci. U.S.A.* **1986**, *83*, 3746–3750.
- (29) Rychlik, W.; Spencer, W. J.; Rhoads, R. E. *Nucleic Acids Res.* **1990**, *18*, 6409–6412.
- (30) Lu, X. C.; Dong, X.; Zhang, K. Y.; Han, X. W.; Fang, X.; Zhang, Y. Z. *Analyst* **2013**, *138*, 642–650.
- (31) Bonanni, A.; Chua, C. K.; Zhao, G. J.; Sofer, Z.; Pumera, M. *ACS Nano* **2012**, *6*, 8546–8551.
- (32) Pylaev, T. E.; Khanadeev, V. A.; Khlebtsov, B. N.; Dykman, L. A.; Bogatyrev, V. A.; Khlebtsov, N. G. *Nanotechnology* **2011**, *22*, 285501.
- (33) Altintas, Z.; Tothill, I. E. *Sens. Actuators, B* **2012**, *169*, 188–194.
- (34) Ganbold, E. O.; Kang, T.; Lee, K.; Lee, S. Y.; Joo, S. W. *Colloids Surf., B* **2012**, *93*, 148–153.
- (35) Dirks, R. M.; Bois, J. S.; Schaeffer, J. M.; Winfree, E.; Pierce, N. A. *SIAM Rev.* **2007**, *49*, 65–88.
- (36) Zuo, X. L.; Song, S. P.; Zhang, J.; Pan, D.; Wang, L. H.; Fan, C. H. *J. Am. Chem. Soc.* **2007**, *129*, 1042–104.
- (37) Lu, Y.; Li, X. C.; Zhang, L. M.; Yu, P.; Su, L.; Mao, L. Q. *Anal. Chem.* **2008**, *80*, 1883–1890.
- (38) Zhang, Y. L.; Huang, Y.; Jiang, J. H.; Shen, G. L.; Yu, R. Q. *J. Am. Chem. Soc.* **2007**, *129*, 15448–15449.
- (39) Radi, A. E.; Ciara K. O'Sullivan, C. K. *Chem. Commun.* **2006**, 3432–3434.
- (40) Hayashi, E.; Takada, T.; Nakamura, M.; Yamana, K. *Chem. Lett.* **2010**, *39*, 454–455.
- (41) Ricci, F.; Lai, R. Y.; Heeger, A. J.; Plaxco, K. W.; Sumner, J. J. *Langmuir* **2007**, *23*, 6827–6834.